Pelagic food web structure in high nutrient low chlorophyll (HNLC) and naturally iron fertilized waters in the Kerguelen Islands region, Southern Ocean

Hunt Brian P.V. [1, 2, 3, *], Espinasse Boris [4], Pakhomov Evgeny A. [1, 2, 3], Cherel Yves [5], Cotté Cedric [6], Delegrange Alice [7, 8], Henschke Natasha [2]

[1] Institute for the Oceans and Fisheries, University of British Columbia, Vancouver, British Columbia, Canada
[2] Department of Earth, Ocean and Atmospheric Sciences, University of British Columbia, Vancouver, British Columbia, Canada
[3] Hakai Institute, Heriot Bay, British Columbia, Canada
[4] Department of Arctic and Marine Biology, UiT The Arctic University of Norway, Tromsø, Norway
[5] Centre d'Etudes Biologiques de Chizé (CEBC), UMR 7372 CNRS- La Rochelle Université, 79360 Villiers-en-Bois, France
[6] Sorbonne Université, CNRS, IRD, MNHN, Laboratoire d'Océanographie et du Climat: Expérimentations et Approches Numériques (LOCEAN-IPSL), Paris, France
[7] Institut National Supérieur du Professorat et de l'Éducation (INSPÉ) - Académie de Lille Hauts-de-France, Site d'Outreau10, rue H. Adam, 62230, Outreau, France
[8] Laboratoire d'Océanologie et de Géosciences - LOG UMR CNRS 8187, Maison de la Recherche en Environnement Naturel 32, Avenue Foch, 62930 Wimereux, France

* Corresponding author : Brian P. V. Hunt, email address : b.hunt@oceans.ubc.ca

Abstract :

The Kerguelen Plateau is a region of natural iron fertilization in the Southern Ocean, within the typically iron limited High Nutrient Low Chlorophyll (HNLC) waters of the eastward flowing Antarctic Circumpolar Current. Between 26 February and 19 March 2018, the MOBYDICK expedition investigated pelagic ecosystem dynamics in the Kerguelen Island region on the northern plateau during the post-phytoplankton bloom period. The survey specifically targeted sampling at two stations in the HNLC waters to the west of the Kerguelen Plateau, and in the iron enriched waters on and to the east of the plateau. A combination of WP2, WP3 and Mesopelagos midwater trawl were used to sample the mesozooplankton (125 µm to ≤10 mm), macrozooplankton (10–30 mm) and micronekton (> 30 to 200 mm) communities. Stable carbon (δ13C) and nitrogen (δ15N) isotopes were measured across representative samples of taxa from all stations. Trophic positions was estimated using a Bayesian isotope mixing model (tRophicPosition), that uses both the δ13C and δ15N values of baselines and consumers. Meso/macrozooplankton trophic positions (TPs) were ~ 2.4 on the plateau and > 0.6 TPs higher at the upstream HNLC stations. This provides empirical evidence for shorter food chains on the diatom dominated plateau and longer food chains in the HNLC region dominated by pico and nanophytopklankon. Meso/macrozooplankton TPs were also elevated downstream of the plateau, though to a lesser extent than in the upstream region, likely reflecting the effect of downstream iron transport, supporting elevated phytoplankton production in the downstream region. There was a consistent increase in trophic position between

meso/macrozooplankton and micronekton of ~0.6 at all stations. Food chain length was therefore determined by the composition of the trophic levels below micronekton. Similar trophic structure at the two upstream HNLC stations, on either side of the northern branch of the Polar Front, indicated that food chain length was robust to the differences in community composition, and supports the critical role of size structured trophic interactions in determining food web properties.

Highlights

► This study used stable isotopes to analyse the pelagic food web structure in the Kerguelen Island region, comparing HNLC areas upstream of the plateau and the iron enriched area on the plateau that experiences a large seasonal phytoplankton bloom. ► Trophic position was calculated for mesozooplankton, macrozooplankton, and micronekton using a Bayesian isotope mixing model approach. ► Meso and macrozooplankton trophic positions were similar but ~0.6 trophic positions lower than micronekton within areas. ► Median meso/macrozooplankton trophic position was ~2.4 on the plateau and 0.6 trophic positions higher in HNLC areas. ► Food chains were longer in HNLC regions, and food chain length was determined by the composition of the trophic levels below micronekton. ► Size based food web structure was robust to differences in community taxonomic composition.

Keywords : zooplankton, micronekton, food web, size structure, stable isotopes, Southern Ocean, Kerguelen Plateau.

Introduction

The Southern Ocean is broadly characterized as a High Nutrient Low Chlorophyll (HNLC) region where productivity is limited by the micronutrient iron (de Baar et al. 1995). Regions of naturally occurring iron enrichment occur in the vicinity of shallow bathymetry (e.g., continental shelf environments and island shelves) or in association with sea ice melt. Such regions are associated with enhanced phytoplankton productivity and can support a high biomass of consumers, for example, South Georgia (Korb et al. 2008) and Kerguelen Islands (Blain et al. 2007). While the physiological mechanisms behind the importance of iron to increased primary productivity are well understood (Olson et al. 2000), and the link to increased food web biomass established (Hindell et al. 2011), few studies have examined the

effect of iron enrichment on the structure and function of Southern Ocean food webs (Stowasser et al. 2012, Tarling et al. 2012).

Pelagic food webs begin with phytoplankton, and here iron availability can play a key role in setting the food web base, impacting the species composition of phytoplankton communities (Hoffmann et al. 2006), their biochemical composition (Hoffmann et al. 2007), and their size structure (Sunda & Huntsman 1997). Size is a particularly important parameter in food web interactions. Synthetic analyses of predator-prey size relationships across terrestrial to marine ecosystems has demonstrated that in > 90% of feeding linkages predators are larger than their prey (Cohen et al. 1993, Barnes et al. 2010). Indeed, in marine ecosystems, body size can be a better predictor of trophic position than an organism's taxonomy (Sheldon et al. 1972, Jennings et al. 2001, Andersen et al. 2016). In the Southern Ocean, phytoplankton in HNLC regions are dominated by cells < 20 μm in size (nano and picophytoplankton) and their annual production can exceed that of larger (> 20 μm) microphytoplankton by a factor of 2.7 (Uitz et al. 2010). By contrast, in regions of natural iron enrichment microphytoplankton dominate and can form extensive and persistent blooms (Blain et al. 2007). Given the fundamental role of size in determining food web interactions, epitomized by the interaction of size and the grazing dynamics of zooplankton functional groups (Fortier et al. 1994), iron driven shifts in phytoplankton size composition may have a significant bearing on Southern Ocean pelagic food web properties.

Based on size structured feeding dynamics, as outlined above, the smaller phytoplankton size classes found in HNLC regions of the Southern Ocean are expected to favour longer food chains than iron enriched areas where large phytoplankton size classes dominate the summer high productivity period. Assuming consistent transfer efficiency between trophic levels, short food chains in iron enriched areas are therefore expected to transfer biomass more efficiently to higher trophic levels than longer food chains in HNLC regions. Food chain length is also influenced by the ratio of predator to prey size (Cousins 1987), with smaller predator-prey mass ratios (PPMR) yielding longer food chains, and vice versa. Furthermore, smaller PPMRs and longer food chains have been found to be associated with more stable environments (Jennings & Warr 2003) and this has potential implications for Southern Ocean food webs. The seasonal amplitude of primary production in HNLC vs naturally iron fertilized regions can vary by an order of magnitude (Blain et al. 2007). We can therefore hypothesise that HNLC regions, with more stable production cycles, would have smaller PPMRs than iron enriched areas, further contributing to elongation of the food chain in these regions.

Stable isotopes provide a valuable tool for empirical analysis of food web properties, including basal resources, organic matter transfer, and food chain length. Carbon and nitrogen are the two elements most commonly measured in food web isotope analyses. Carbon isotopes ($\delta^{13}C$) are typically enriched by ~ 0.5-1 ‰ and nitrogen isotopes ($\delta^{15}N$) by ~ 3.4 ‰ per trophic level in any given food web. The signature of a food webs basal resources (primary producers) are therefore more strongly conserved in consumer $\delta^{13}C$ values, and carbon isotopes have most frequently been used to trace and identify these food web sources (Minagawa & Wada 1984,

Vander Zanden & Rasmussen 2001, Post 2002, McCutchan et al. 2003). Conversely, nitrogen

isotopes are most frequently used to estimate the trophic position of food web components,

which can be further extrapolated to food chain length. The calculation of trophic position and

food chain length from isotope values is complicated by variability / uncertainty in key values,

including trophic enrichment factors, baselines, and consumers, and the associated error

propagation through estimates. However, the development of Bayesian approaches have

overcome some of these limitations, while also taking into account both $\delta^{15}N$ and $\delta^{13}C$ in

trophic position estimates (Phillips et al. 2014, Quezada-Romegialli et al. 2018).

The Kerguelen plateau represents an ideal region to investigate the role of natural iron

fertilization in structuring pelagic food webs in the Southern Ocean. The plateau extends south-

east of the Kerguelen Islands, and has a shallow bathymetry (< 700 m) that represents a major

obstacle to the Antarctic Circumpolar Current (ACC) (Park et al. 2008). Circulation interactions

with the shallow topography transport iron to the surface waters of the plateau where a bloom

routinely forms between November and February, with an areal extent of up to 45,000 km^2

(Blain et al. 2007, Mongin et al. 2008). From February to March 2018, the "Marine Ecosystem

Biodiversity and Dynamics of Carbon around Kerguelen" program, hereafter referred to as

MOBYDICK, set out to research contrasting productivity regimes in the Kerguelen region during

the post-bloom period. The MOBYDICK expedition builds upon three previous programs in the

area: the Kerguelen Ocean and Plateau compared Study (KEOPS) in summer 2005, KEOPS2 in

spring 2011, and the "Myctophid assessment in relation to Oceanographic conditions: a three

Dimension Density Distribution approach combining Modelling, Acoustic-and Predators'" data

(MyctO-3D-MAP) in summer 2014. The MOBYDICK station positions were selected to coincide with areas sampled during these previous surveys and included one station on the plateau (iron enriched), two stations to the west of the plateau (iron limited), and one station to the east of the plateau (iron enriched).

According to size structured feeding dynamics and stability driven decreases in PPMR, we predict that iron rich regions, dominated by large microphytoplankton and large amplitude blooms, would have shorter food chains than iron limited regions dominated by smaller phytoplankton size classes and lower amplitude blooms. To test this prediction, we used 1) stable isotope data collected during the MOBYDICK expedition to estimate the trophic position of the mesozooplankton, macrozooplankton and micronekton components of the pelagic food web; 2) and specifically compared trophic position estimates of these food web components between iron enriched and iron limited regions in the vicinity of the Kerguelen Plateau. These measurements are expected to provide new insights into the role of iron supply in pelagic food web structure and function in the Southern Ocean, with implications for materials flux.

Methods

Sampling during the MOBYDICK expedition was completed aboard the *Marion Dufresne II* from 26 February to 19 March 2018. The location of the four stations sampled is indicated in Figure 1. Station M2 was located on the plateau, and was the "bloom" reference station A3 in KEOPS and KEOPS2. Station M3, located to the west of the plateau, corresponded to the KERFIX

7

station of KEOPS, and M4, also west of the plateau, was located roughly 100 nautical miles south of the HNLC reference stations of KEOPS2 (Blain et al., 2015). Repeat sampling was conducted at stations M2, M3, and M4 (Table 1). Station M1 was located east of Kerguelen, in the core foraging area of the Kerguelen king penguin population (Scheffer et al., 2016), and was only sampled once.

Sample collection

Particulate organic matter (POM) was sampled in conjunction with each WP2+3 zooplankton net deployment, collected from the ship-board sea water line from a depth of ~ 10 m. Approximately 2 L of water was filtered onto a 25 mm pre-combusted GF/F filter by vacuum filtration. Mesozooplankton were sampled with a WP2 net (2.5 m long, 57 cm diameter) fitted with 200 μm mesh and deployed to a depth of 200 m. Macrozooplankton were collected with a WP3 net (2 m long, 1.13 m diameter) fitted with 1000 μm mesh. The WP2 and WP3 were deployed once during the night at station M1, and once each during the day and night on each visit to stations M2-M4. Three daytime and three nighttime trawls were conducted on each visit to all stations using a Mesopelagos trawl designed by Ifremer (Fisheries Biology and Technology Laboratory, LTBH, Lorient, France) (Meillat 2012). This non-closing trawl has vertical and horizontal openings which vary between 5 and 6 m and 10 and 12 m, respectively. The trawl has a mesh size of 40 mm in the wings, reducing to 5 mm in the codend. A Scanmar acoustic device (Åsgårdstrand, Norway) was attached to the net for real time monitoring of trawl depth simultaneously with acoustic measurements (Williams & Koslow 1997). Sampling depths were

dependent on acoustic backscatter, with trawls targeting areas of high backscattering signals in shallow, middle and deep layers (Table 1). During trawling, the vessel maintained a speed of 1.5 m s^{-1} while fishing the target depth for ~30 minutes. The trawl was deployed and retrieved as fast as possible to ensure that organisms were mainly caught at the targeted depth.

Sample processing

The WP2 net samples were size fractionated into 6 size classes with a sieve column: 125-250, 250-500, 500-1000, 1000-2000, 2000-4000, and > 4000 μm. The size fractions < 4000 μm were filtered onto 47 mm pre-combusted and pre-weighed GF/F filters by vacuum filtration and then oven dried at 50°C for 48 hours onboard the vessel. The > 4000 μm size fraction was separated into species, and specimens measured, grouped into logarithmic size bins, and dried at 50°C for 48 hours onboard the vessel. Macrozooplankton and micronekton were sampled from the midwater trawls with the aim to have representation of major taxa and size classes from all trawls. All individuals were measured to the nearest 1 mm. In the case of smaller animals (< 50 mm), the entire animal was collected. In the case of larger animals, a muscle tissue sample (~ 20 mg) was collected. All samples were oven dried for 48 hours at 50°C onboard the vessel. Once returned to the laboratory all samples were weighed to the nearest 0.01 mg.

Isotope analysis

Samples were not treated to remove lipids or inorganic carbon prior to stable isotope analysis.

Stable carbon and nitrogen elemental and isotopic compositions for all organisms were

measured at the University of Victoria Isotope Facility using a Costech 4010 elemental analyzer

(Costech, Florence) coupled via continuous flow to a Thermo Finnegan Delta Advantage isotope

ratio mass spectrometer (Thermo-Finnigan, Bremen, Germany). Stable isotope values were

expressed in standard δ (‰) notation and a two-point calibration anchored with internal

reference materials ('Caffeine' and 'Dorm', themselves determined using IAEA N1, N2, and CH-6

as well as NBS-22; ESM Table S1) was used to calibrate $\delta^{13}C$ and $\delta^{15}N$ relative to Pee Dee

Belemnite for carbon and Air for nitrogen. Standard deviations for calibration standards for $\delta^{13}C$

and $\delta^{15}N$, respectively, were ± 0.3 ‰ and ± 0.2 ‰ for Caffeine (n=3) and ± 0.3 ‰ and ± 0.2 ‰

for Dorm (n=5). Carbon isotope values were lipid corrected according to individual organism

C:N ratios, using the equation from (Hoffman & Sutton 2010) for fish and from (Smyntek et al.

2007) for invertebrates.

Trophic position calculation

When applying bulk isotopes to estimate food web properties an isotope baseline is required as

an anchor point. The isotopic value of POM has frequently been used as representative of

phytoplankton. However, this value can have high temporal variability, showing rapid response

(days) to fluctuations in nutrients and phytoplankton growth rates (Lorrain et al. 2015), while

also being influenced by non-phytoplankton particulates, including faecal pellets (Checkley &

Entzeroth 1985) and microzooplankton. An alternative approach to establishing a trophic

10

baseline is to use the isotopic value of a primary consumer. Salps (tunicates) have been used in

a number of studies (Post 2002, Cherel et al. 2010, Stowasser et al. 2012). However, recent

analysis has identified salps as unreliable baseline measures due to their unique feeding biology

(Pakhomov et al. 2019). For this study we have used the isotope values of the zooplankton size

classes ≤ 1000 μm as the trophic baseline. Since no zooplankton can be considered to be truly

herbivorous, we assigned a trophic level of 2.25 to this group to take into account a degree of

omnivory.

The species sampled, and the number of animals sampled per species, varied between stations.

To optimize the comparability of sample sets among stations for trophic positon calculation, the

data set was filtered to include only taxa that were common to all stations (see Figure 4). *Salpa*

thompsoni were not included in the trophic position analysis due to uneven sample size, and

their unique trophic ecology, and they are rather discussed separately. Common taxa, excluding

S. thompsoni, were grouped into the length-based groups of mesozooplankton (125 μm to ≤ 10

mm), macrozooplankton (10 30 mm), micronekton (> 30 to 200 mm) (see Table s1 for sample

sizes). Trophic positions were calculated using a one-source, two-isotope (carbon and nitrogen)

Bayesian isotope mixing model implemented with the tRophicPosition package (version 0.7.7,

Quezada-Romegialli et al., 2018) in R (R Core Team 2020). The benefits of this approach are that

it explicitly includes individual variability and propagation of sampling error (trophic enrichment

factors, and measurements of baselines and consumers) in the modelling approach and

posterior estimates of parameters. We used Post's (2002) trophic enrichment factor values of

3.4 ± 0.98 (mean ± standard deviations) for $\delta^{15}N$ and 0.39 ± 1.3 for $\delta^{13}C$. The Bayesian model

11

ran 20,000 iterations for the adaptive phase, 20,000 iterations as burnin (iterations discarded at

the beginning of posterior sampling) and 20,000 actual iterations. The model used five parallel

Markov Chain Monte Carlo(MCMC) simulations using the JAGS (ver. 4.3.0) Gibbs sampler

(Plummer 2003). The median posterior trophic positions are presented showing the 95%

credibility intervals. We then conducted pairwise comparisons of the posterior distributions

among classes with a logical test that one was greater (>) than the other, randomly sampling

posterior distributions until all posterior estimates were compared. The probability that one

class had a higher trophic level than the other increased as the value approached 1. Finally, the

Bhattacharyya coefficient was used to calculate the probability of overlap between two

distributions, with the probability increasing toward 1 (Quezada-Romegialli et al. 2018).

Results

Water mass tracking, described in detail in Henschke et al. (2021), estimated retention times of

≥ 60 days at all sites (Table 2). This suggests that the same water masses were sampled during

each repeat visit to stations M2, M3 and M4. Mixed layer depth was lowest at M1 (27m) and

ranged between 50 and 90 m on repeat visits to the other stations. Mean MLD phytoplankton

biomass was highest at station M2-3 (0.58 µg L^{-1}), but was generally < 0.3 µg L^{-1}. A large

phytoplankton bloom was observed at Stations M1 and M2 in December – January, two to

three months prior to the MOBYDICK expedition, where phytoplankton biomass exceeded 2 µg

L^{-1} (Figure s1). Elevated phytoplankton biomass was also observed at the upstream stations M3

and M4 at this time, through levels were substantially lower (~ 0.5 µg L^{-1}). Mixed layer water

temperature was highest at station M3. The absence of a temperature minimum at 200 m at M3 confirmed that it was conducted north of the APF, whereas M1, M2 and M4 stations were located south of the APF in the Antarctic Zone (Henschke et al. 2021). Zooplankton biomass was lowest at stations M1 and M3-1 (~ 5 mgC m^{-3}) and averaged 10.84 mgC m^{-3} across all other stations with a maximum of 13.65 mgC m^{-3} at Station M4-1. Highest values of crustacean biomass were observed at M2, while the highest fish biomass was observed at M3.

Trophic positions were calculated using station specific δ^{13}C and δ^{15}N values of zooplankton size classes ≤ 1000 μm as the trophic baseline. Comparison with other baseline proxies showed that zooplankton had lower within site variability than either POM or *Salpa thompsoni*, and that δ^{15}N values had the least variability within stations (Figure 2). Carbon isotope values (Figure 2A) were highest at M2 (average = -23.4 ‰) and lowest at M3 (ave. = -25.3 ‰) and M4 (ave. = -26.2 ‰). A decreasing trend over time in zooplankton δ^{13}C values was evident at M2 and M3. The δ^{13}C values of *S. thompsoni* generally followed the same pattern as POM. Nitrogen isotope values of zooplankton (Figure 2B) were highest at M2 (ave. = 2.3 ‰), followed by M1 (ave. = 0.9 ‰), and were lowest at M3 (ave. = -0.1) and M4 (ave. = 0.1). The δ^{15}N values of zooplankton decreased slightly over time at M2. A much stronger decreasing trend was apparent for POM and *S. thompsoni* at M2, likely reflecting the higher tissue turnover rates of these groups relative to zooplankton.

The mesozooplankton size class largely comprised zooplankton from the WP2 net size fractions ≤ 2000 μm and copepods (Figure 3A). Both the macrozooplankton and micronekton included a

13

mix of gelatinous and non-gelatinous taxa. Macrozooplankton included pteropods (gymnosomes and thecosomes), siphonophores, hydrozoans, gammarids, mysids, and euphausiids. Micronekton included squid, decapods, scyphozoans, tunicates, fish, chaetognaths and ctenophores. Nitrogen isotopes values typically increase with trophic level which is expected to correlate with organism size. This was largely the case in this study, and fish, which included the largest individuals, had the highest median δ^{15}N values (Figure 3B). However, the large gelatinous taxa of tunicates, chaetognaths and ctenophores all had low δ^{15}N values relative to their size. This was at least expected for the small particle grazing tunicates, which in this case comprised entirely of *Salpa thompsoni* (Figure 2). The widest range of δ^{15}N values was observed for copepods, indicating diverse foraging strategies in this group.

Mean δ^{15}N values are presented for the 20 taxa used in the posterior trophic position analysis, as well as the tunicate *S. thompsoni* (Figure 4). Overall, δ^{15}N values increased with organism size for all taxa. *Salpa thompsoni* consistently had the lowest δ^{15}N values, and interestingly the hyperiid amphipods *Cyllopus magellanicus* and *Vibilia antarctica* both had low δ^{15}N values, suggesting predation on *S. thompsoni*. The myctophid *Electrona antarctica* had the highest δ^{15}N values, indicating that this species had the highest trophic level. Values of δ^{13}C also generally increased with size, although this trend was not as apparent as for δ^{15}N.

The three organism size classes of mesozooplankton, macrozooplankton, and micronekton showed a consistent pattern of posterior trophic positions (PTP). Mesozooplankton and macrozooplankton were always similar with the greatest difference in trophic position between

14

these classes being 0.16 at station M4 (Figure 5; Table s2). The median PTP of meso /

macrozooplankton was 0.74 PTPs higher at M3 than M2, 0.62 PTPs higher at M4 than M2, and

0.41 PTPs higher at M1 than M2. Micronekton were on average 0.57 trophic positions higher

than meso / macrozooplankton and micronekton, with the greatest difference being 0.81

trophic positions at station M4. PTPs were lowest at M2, with an average of 2.4 for meso and

macrozooplankton. Pairwise comparison of PTPs found high probability (0.9-1) that PTPs were

greater at stations M1, M3 and M4 than M2 (Table 3), and a high probability that PTPs were

greater at M3 and M4 than M1. The probability of overlap of PTP distributions was low

between M2 and stations M3 and M4, being < 0.3 except for M4 mesozooplankton vs M2 meso

/ macrozooplankton (~ 0.4; Table 4). This provided further support for the distinct, higher, PTPs

in the upstream vs plateau stations. The probability of overlap between station M1 and all

other stations was generally > 0.55, demonstrating that the downstream region was

intermediate in PTP characteristics between the plateau and upstream region.

Discussion

The Kerguelen Islands and plateau are a region of natural iron fertilization within the typically

iron limited High Nutrient Low Chlorophyll (HNLC) waters of the eastward flowing Antarctic

Circumpolar Current. The MOBYDICK expedition provided an opportunity to investigate the

effect of iron enhanced productivity on the structure and function of the lower trophic levels of

the Southern Ocean food web, at the end of the summer phytoplankton bloom. This study

sampled the mesozooplankton, macrozooplankton, and micronekton food web in the HNLC

15

waters to the west of the Kerguelen Plateau, in the iron enriched waters on the plateau, and

the waters east of the plateau which are iron enriched by off-plateau advection (d'Ovidio et al.

2015). Using bulk carbon and nitrogen stable isotope we demonstrated that the trophic

positions of meso and macrozooplankton were > 0.6 trophic levels higher at the upstream HNLC

stations than on the plateau, and were also elevated downstream of the plateau, though to a

lesser extent. This supported the prediction that the iron rich plateau would have a shorter

food chain than the iron limited upstream region, and that the downstream region had

enhanced production due to iron enrichment from the plateau. Below we discuss our findings

in the context of the Kerguelen region pelagic ecosystem dynamics, and the implications for

energy flow in the contrasting productivity regimes.

The MOBYDICK expedition took place in the post-bloom period of the seasonal production cycle

and phytoplankton biomass was low in all sampled areas (< 0.6 μgL^{-1}), but lowest upstream of

the plateau (< 0.22 μgL^{-1}). However, satellite observations showed that in December / January

prior to the expedition phytoplankton biomass reached a peak of > 2 μgL^{-1} over the plateau

region where station M2 was located, and downstream (east) of the plateau, highlighting the

effect of natural iron fertilization. The seasonal bloom cycle and spatial extent observed in 2018

were consistent with observations in previous years, indicating that this is a recurring feature of

the region (Blain et al. 2007, Laurenceau-Cornec et al. 2015). The HNLC region upstream of the

Kerguelen Plateau is broadly representative of the Southern Ocean and is dominated by small

phytoplankton, with picophytoplankton comprising up to 50% and nanophytoplankton > 20%

(mostly *Phaeocystis* and small diatoms, e.g., *Fragilariopsis*) of the total biomass (Fiala et al.

16

1998, Lasbleiz et al. 2016). Conversely, blooms over the plateau are dominated by large diatoms and smaller chain forming diatoms such as *Pseudonitzschia* and *Chaetoceros* (Lasbleiz et al. 2016). In the post-bloom period sampled during MOBYDICK, Prymnesiophytes, dominated by *Phaeocystis antarctica* (3 μm cell size), were the most abundant phytoplankton group, representing up to 53% and 70% of the Chl-a on and off the plateau, respectively (Irion et al. 2020). Small diatoms, e.g., *Fragilariopsis* and *Chaetoceros*, were abundant at stations M4 and M1, while M3 had the lowest contribution of diatoms (25% of Chl-a), likely due to silicate and iron co-limitation. On the plateau, large diatoms, e.g., *Coretkron* dominated in low silicate post-bloom conditions in the mixed layer. Below the mixed layer, large and heavily silicified diatoms were abundant (e.g., *Eucampia* and *Odontella*).

Preliminary analysis of the zooplankton community composition during MOBYDICK found greatest similarity between stations M1 and M4, and that both of these stations overlapped in composition with M2 (Figure s4 and s5), i.e., there was not a distinct separation of the plateau zooplankton community from that upstream (M4) and downstream (M1). Station M3 showed the greatest dissimilarity to other stations, reflecting differences in the community composition north and south of the northern branch of the Polar Front (Figure 1). Copepods, particularly *Oithona* and Calanoids, dominated abundance at all stations (Figure s2 and s3), in agreement with the KEOPS surveys where copepods contributed > 80 % to total mesozooplankton abundance (Carlotti et al. 2008, Carlotti et al. 2015). Despite similarities in zooplankton community composition to M1 and M4, plateau station M2 did record the highest crustacean and gelatinous zooplankton biomass, indicating a positive response to higher phytoplankton

17

productivity in this region. However, there was substantial variation in zooplankton biomass among stations during MOBYDICK. While areal mesozooplankton biomass during MOBYDICK was an order of magnitude higher (1-2.7 gC m^{-2}) than recorded in November (0.25 – 0.49 gCm^{-2}) during the KEOPS2 survey (Carlotti et al. 2015), it was up to an order of magnitude lower than during the January / February KEOPS survey (3.44 – 19.26 gCm^{-2}) (Carlotti et al. 2008). Although the February / March sampling dates of the MOBYDICK expedition coincided with the period of peak zooplankton biomass observed during the YugNIRO times-series in 1987 / 88 (Hunt et al. 2011), seasonal Continuous Plankton Recorder data collected across the Sub-Antarctic and Polar Frontal zones in 2001 / 2002 found a peak of zooplankton abundance in February (Hunt & Hosie 2006). The seasonal timing of the zooplankton peak biomass likely varies interannually, however, based on the December / January phytoplankton bloom timing in 2018 (Figure s1), zooplankton biomass observed during MODYDICK was probably declining after the summer peak (Semelkina 1993, Razouls et al. 2006, Hunt et al. 2011).

The combined sampling methods conducted during MODYDICK provided an opportunity to collect stable isotope data for the mesozooplankton, macrozooplankton and micronekton components of HNLC and naturally iron fertilized water masses in the Kerguelen plateau region. An important consideration when evaluating these data was whether the stable isotope ratios measured were representative of the food web history within the sampled water mass. This would depend on the water mass retention time in the areas sampled and the tissue turnover rates of the organisms. Water mass tracking estimated water mass residence times of at least 60 days in each of the areas sampled by the four stations (Henschke et al. 2021). Organism

tissue turnover rates scale with organism size and growth rate (Fry & Arnold 1982, Hesslein et al. 1993). The highest turnover rates, and most rapid response to changing food web conditions (e.g., nitrate supply), are therefore expected to occur in particulate organic matter (POM). Laboratory studies indicate that diatom isotope replacement rates can be on the order of days (Montoya & McCarthy 1995). Few mesocosm studies have been conducted for Southern Ocean zooplankton, with one study reporting tissue turnover rates for *Euphausia superba* of 54% for nitrogen after 30 days (Schmidt et al. 2003). However, it is expected that warmer water Sub-Antarctic and Antarctic Zone zooplankton during the growing season would have higher turnover rates. Fry and Arnold (1982) reported turnover rates for shrimp and brine shrimp of 4-19 days. In our study, there was evidence for a temporal decline in stable isotope values of POM, *S. thompsoni* and < 1000 μm zooplankton over the three visits to M2, which spanned three weeks. In the case of micronekton, turnover rates are expected to be weeks to months (Hesslein et al. 1993, Colborne et al. 2017). Given the estimated water mass residence times for the study area, it is reasonable to expect that the measured stable isotope ratios of most taxa were representative of the food web history within the water mass in which they were sampled, including the pre-voyage bloom conditions.

The elevated on-plateau δ^{15}N values of the stable isotope baseline used in this study, zooplankton < 1000 μm, reflected the higher productivity in this region. Phytoplankton δ^{15}N values increase in response to nitrate competition during high productivity periods (Altabet & Francois 2001), and these elevated δ^{15}N values were transmitted to the zooplankton on the plateau. Using a Bayesian modelling approach, that applied both carbon and nitrogen isotopes

values of baselines and consumers, we estimated that the trophic positions of meso and macrozooplankton were > 0.6 higher at the upstream HNLC stations than on the plateau. This result provided empirical support for the prediction that iron rich regions, dominated by large microphytoplankton and large amplitude blooms, would have shorter food chains than iron limited regions dominated by smaller phytoplankton and lower amplitude blooms. The dominance of pico and nanophytoplankton in the HNLC upstream region favours a prominent role of heterotrophic nanoflagellates and ciliates as trophic intermediaries between phytoplankton and zooplankton (Sommer et al. 2002), and a longer food chain. The lower amplitude seasonal phytoplankton bloom, and hence more stable production cycle in HNLC regions may also contribute to elongation of the food chain through favouring smaller predator-prey mass ratios (Jennings & War 2005). Conversely, the iron enriched plateau favours diatom blooms and direct consumption of phytoplankton by zooplankton. Indeed, a higher degree of herbivory was observed for meso and macrozooplankton on the plateau than off the plateau. The shorter plateau food chain promotes more efficient biomass transfer to higher trophic levels, and augmented by higher primary productivity is expected to yield enhanced on-plateau biomass accumulation. The region downstream of the plateau had meso and macrozooplankton trophic positions intermediate between the upstream and plateau region, reflecting the effect of downstream iron transport which fuels the elevated phytoplankton production in the downstream region (Blain et al. 2007).

The trophic position analysis identified two additional important features of the trophic structure in the study area. Firstly, the meso and macrozooplankton components of the food

chain had a high degree of the trophic position overlap that was independent of whether the community was in an HNLC or productive plateau region. The mean trophic position of meso and macrozooplankton on the plateau was 2.4, indicating a similar contribution of herbivory and carnivory in these size classes. The presence of large macrozooplankton grazers, such as euphausiids, may be a key factor in the effective grazing and transfer of large diatom biomass to higher trophic levels when blooms occur. There is evidence that diatoms are selected against by some zooplankton grazers, while their silicified cell walls limit the number of grazers that are capable of consuming and assimilating them (Verity & Smetacek 1996, Liu et al. 2016). The higher trophic position (~ 3) of both meso and macrozooplankton in the off-plateau areas indicted that these taxa switched to increased carnivory when large diatoms were less abundant. Secondly, there was a consistent increase in trophic position between meso / macrozooplankton and micronekton of ~ 0.6 at all stations. Food chain length was therefore determined by the composition of the trophic levels below micronekton. The similarity of trophic structure at the two upstream stations, M3 and M4, indicated that food chain length was robust to the differences in community composition that occurred across the northern branch of the Polar Front. This supports the critical role of size structured trophic interactions in determining food web properties.

While size was clearly related to trophic level in our study, with the smallest organisms (mesozooplankton) having the lowest trophic level and the largest organisms (fish) the highest, wide isotopic ranges for some groups reflected diverse within group feeding ecologies. For example, copepods spanned approximately two trophic levels, including the carnivorous genus

Paraeuchaeta and herbivorous species such as *Rhincalanus gigas*. Wide isotopic ranges were also observed for other groups, including Hydrozoans, Decapods, Chaetognaths and Hyperiids. The trophic diversity of taxa within the lower levels of pelagic food webs is an important consideration when parameterizing food web models, where the lower trophic levels are frequently aggregated into a few groups with constrained functional roles. *Salpa thompsoni* was a major exception to the size rule, being one of the largest taxa but with δ^{15}N values lower than the mesozooplankton, indicating a lower trophic level. Size fractionated particulate organic matter (POM) analyses show that, as with the rest of the food web, POM stable isotope values scale with size, and that this is particularly evident in δ^{15}N values (Trull et al. 2015). *Salpa thompsoni's* low δ^{15}N values in our study underscore their unique functional role as large bodied small particle grazers. Due to salps ability to effectively filter extremely small particles (< 1 μm) they can separate from the classical food web (Vargas & Madin 2004, Pakhomov et al. 2019). Notably, the hyperiid amphipod *Cyllopus magellanicus* and *Vibilia antarctica* both had low δ^{15}N values, particularly at station M1 where *S. thompsoni* was most abundant (Henschke et al. 2021). Both species are known commensals of *S. thompsoni* and therefore it is highly likely that these hyperiids predated on *S. thompsoni*, providing an indirect pathway for *S. thompsoni* biomass into the pelagic food web.

Summary

Shifts in the size structure of phytoplankton at the food web base determine trophic pathways, and the number of trophic steps leading to mesozooplankton and macrozooplankton, and by

extension the efficiency of biomass transfer to higher trophic levels. We found that HNLC waters upstream of the Kerguelen plateau, dominated by pico and nanophytoplankton, had mesozooplankton / macrozooplankton communities that were > 0.6 trophic positions higher than on the naturally iron enriched plateau which supports large summer diatom blooms. Mesozooplankton / macrozooplankton in the region downstream of the plateau were intermediate in trophic position between the upstream and plateau regions, indicting the effect of iron enrichment though downstream transport from the plateau. Food chain length was determined by the composition of interactions between trophic levels below the micronekton, which were consistently ~ 0.6 trophic positions above meso / macrozooplankton at all stations. We suggest that the efficiency of biomass accumulation in iron enriched regions depends on the presence of large zooplankton grazers that are able to effectively consume and assimilate diatoms, e.g., euphausiids. We also note the high trophic diversity of lower trophic level taxa, which supports a more nuanced approach to structuring food web models, and more effectively represent the diverse functional roles of these taxa.

Acknowledgements

Declaration of interests

The authors declare that they have no known competing financial interests or personal relationships

that could have appeared to influence the work reported in this paper.

References

Altabet MA, Francois R (2001) Nitrogen isotope biogeochemistry of the Antarctic Polar Frontal Zone at 170°W. Deep Sea Research Part II: Topical Studies in Oceanography 48:4247-4273

Andersen KH, Berge T, Gonçalves RJ, Hartvig M, Heuschele J, Hylander S, Jacobsen NS, Lindemann C, Martens EA, Neuheimer AB, Olsson K, Palacz A, Prowe AE, Sainmont J, Traving SJ, Visser AW, Wadhwa N, Kiørboe T (2016) Characteristic Sizes of Life in the Oceans, from Bacteria to Whales. Annual Reviews in Marine Science 8:217-241

Barnes C, Maxwell D, Reuman DC, Jennings S (2010) Global patterns in predator-prey size relationships reveal size dependency of trophic transfer efficiency. Ecology 91:222-232

Blain S, Quéguiner B, Armand L, Belviso S, Bombled B, Bopp L, Bowie A, Brunet C, Brussaard C, Carlotti F, Christaki U, Corbière A, Durand I, Ebersbach F, Fuda J-L, Garcia N, Gerringa L, Griffiths B, Guigue C, Guillerm C, Jacquet S, Jeandel C, Laan P, Lefèvre D, Lo Monaco C, Malits A, Mosseri J, Obernosterer I, Park Y-H, Picheral M, Pondaven P, Remenyi T, Sandroni V, Sarthou G, Savoye N, Scouarnec L, Souhaut M, Thuiller D, Timmermans K, Trull T, Uitz J, van Beek P, Veldhuis M, Vincent D, Viollier E, Vong L, Wagener T (2007) Effect of natural iron fertilization on carbon sequestration in the Southern Ocean. Nature 446:1070-1074

Carlotti F, Jouandet MP, Nowaczyk A, Harmelin-Vivien M, Lefèvre D, Richard P, Zhu Y, Zhou M (2015) Mesozooplankton structure and functioning during the onset of the Kerguelen phytoplankton bloom during the KEOPS2 survey. Biogeosciences 12:4543-4563

Carlotti F, Thibault-Botha D, Nowaczyk A, Lefèvre D (2008) Zooplankton community structure, biomass and role in carbon fluxes during the second half of a phytoplankton bloom in the eastern sector of the Kerguelen Shelf (January–February 2005). Deep Sea Research Part II: Topical Studies in Oceanography 55:720-733

Checkley DM, Jr., Entzeroth LC (1985) Elemental and isotopic fractionation of carbon and nitrogen by marine, planktonic copepods and implications to the marine nitrogen cycle. Journal of Plankton Research 7:553-568

Cherel Y, Camille Fontaine, Pierre Richard, Labat J-P (2010) Isotopic niches and trophic levels of myctophid fishes and their predators in the Southern Ocean. Limnology and Oceanography 55:324-332

Cohen JE, Pimm SL, Yodzis P, Salda J (1993) Body Sizes of Animal Predators and Animal Prey in Food Webs. Journal of Animal Ecology 62:67-78

Colborne SF, Fisk AT, Johnson TB (2017) Tissue-specific turnover and diet-tissue discrimination factors of carbon and nitrogen isotopes of a common forage fish held at two temperatures. Rapid Communications in Mass Spectrometry 31:1405-1414

Cousins S (1987) The decline of the trophic level concept. Trends in Ecology & Evolution 2:312-316

d'Ovidio F, Della Penna A, Trull TW, Nencioli F, Pujol MI, Rio MH, Park YH, Cotté C, Zhou M, Blain S (2015) The biogeochemical structuring role of horizontal stirring: Lagrangian perspectives on iron delivery downstream of the Kerguelen Plateau. Biogeosciences 12:5567-5581

de Baar HJW, de Jong JTM, Bakker DCE, Löscher BM, Veth C, Bathmann U, Smetacek V (1995) Importance of iron for plankton blooms and carbon dioxide drawdown in the Southern Ocean. Nature 373:412-415

Donlon CJ, Martin M, Stark J, Roberts-Jones J, Fiedler E, Wimmer W (2012) The Operational Sea Surface Temperature and Sea Ice Analysis (OSTIA) system. Remote Sensing of Environment 116:140-158

Fiala M, Semeneh M, Oriol L (1998) Size-fractionated phytoplankton biomass and species composition in the Indian sector of the Southern Ocean during austral summer. Journal of Marine Systems 17:179-194

Fortier L, Le Fevre J, Legendre L (1994) Export of biogenic carbon to fish and to the deep ocean: the role of large planktonic microphages. Journal of Plankton Research 16:809-839

Fry B, Arnold C (1982) Rapid 13C/12C turnover during growth of brown shrimp (Penaeus aztecus). Oecologia 54:200-204

Henschke N, Blain S, Cherel Y, Cotte C, Espinasse B, Hunt BPV, Pakhomov EA (2021) Population demographics and growth rate of *Salpa thompsoni* on the Kerguelen Plateau. Journal of Marine Systems 214:103489

Hesslein RH, Hallard KA, Ramlal P (1993) Replacement of Sulfur, Carbon, and Nitrogen in Tissue of Growing Broad Whitefish (Coregonus nasus) in Response to a Change in Diet Traced by δ^{34}S, δ^{13}C, and δ^{15}N. Canadian Journal of Fisheries and Aquatic Sciences 50:2071-2076

Hindell MA, Bost CA, Charrassin JB, Gales N, Lea MA, Goldsworthy S, Page B, Robertson G, Wienecke W, O'Toole M, Guinet C Foraging habitats of top predators, and areas of ecological significance, on the Kerguelen Plateau. In: Duhamel GaW, D., (ed). Proc The Kerguelen Plateau: marine ecosystem and fisheries. Société d'Ichtyologie

Hoffman JC, Sutton TT (2010) Lipid correction for carbon stable isotope analysis of deep-sea fishes. Deep Sea Research Part I: Oceanographic Research Papers 57:956-964

Hoffmann LJ, Peeken I, Lochte K (2007) Effects of iron on the elemental stoichiometry during EIFEX and in the diatoms *Fragilariopsis kerguelensis* and *Chaetoceros dichaeta*. Biogeosciences 4:569-579

Hoffmann LJ, Peeken I, Lochte K, Assmy P, Veldhuis M (2006) Different reactions of Southern Ocean phytoplankton size classes to iron fertilization. Limnology and Oceanography 51:1217-1229

Hunt BPV, Hosie GW (2006) The seasonal succession of zooplankton in the Southern Ocean south of Australia, part II: The Sub-Antarctic to Polar Frontal Zones. Deep Sea Research Part I: Oceanographic Research Papers 53:1203-1223

Hunt BPV, Pakhomov EA, Williams R (2011) Comparative analysis of 1980's and 2004 macrozooplankton composition and distribution in the vicinity of Kerguelen and Heard Islands: seasonal cycles and oceanographic forcing of long-term change. CYBIUM 35:75-92

Irion S, Jardillier L, Sassenhagen I, Christaki U (2020) Marked spatiotemporal variations in small phytoplankton structure in contrasted waters of the Southern Ocean (Kerguelen area). Limnology and Oceanography 65:2835-2852

Jennings S, Pinnegar JK, Polunin NVC, Boon TW (2001) Weak cross-species relationships between body size and trophic level belie powerful size-based trophic structuring in fish communities. Journal of Animal Ecology 70:934-944

Jennings S, Warr KJ (2003) Smaller predator-prey body size ratios in longer food chains. Proceedings of the Royal Society of London Series B: Biological Sciences 270:1413-1417

Korb RE, Whitehouse MJ, Atkinson A, Thorpe SE (2008) Magnitude and maintenance of the phytoplankton bloom at South Georgia: a naturally iron-replete environment. Marine Ecology Progress Series 368:75-91

Lasbleiz M, Leblanc K, Armand LK, Christaki U, Georges C, Obernosterer I, Quéguiner B (2016) Composition of diatom communities and their contribution to plankton biomass in the naturally iron-fertilized region of Kerguelen in the Southern Ocean. FEMS Microbiology Ecology 92

Laurenceau-Cornec EC, Trull TW, Davies DM, Bray SG, Doran J, Planchon F, Carlotti F, Jouandet MP, Cavagna AJ, Waite AM, Blain S (2015) The relative importance of phytoplankton aggregates and zooplankton fecal pellets to carbon export: insights from free-drifting sediment trap deployments in naturally iron-fertilised waters near the Kerguelen Plateau. Biogeosciences 12:1007-1027

Liu H, Chen M, Zhu F, Harrison PJ (2016) Effect of Diatom Silica Content on Copepod Grazing, Growth and Reproduction. Frontiers in Marine Science 3

Lorrain A, Graham BS, Popp BN, Allain V, Olson RJ, Hunt BP, Potier M, Fry B, Galván-Magaña F, Menkes CE (2015) Nitrogen isotopic baselines and implications for estimating foraging habitat and trophic position of yellowfin tuna in the Indian and Pacific Oceans. Deep Sea Research Part II: Topical Studies in Oceanography 113:188-198

McCutchan JH, Lewis WM, Kendall C, McGrath CC (2003) Variation in trophic shift for stable isotope ratios of carbon, nitrogen, and sulfur. Oikos 102:378-390

Meillat M (2012) Essais du chalut mesopelagos pour le programme MYCTO 3D-MAP de l'IRD, a bord du Marion Dufresne (du 19 au 21 aout 2012). .

Minagawa M, Wada E (1984) Stepwise enrichment of 15N along food chains: Further evidence and the relation between $\delta^{15}N$ and animal age. Geochimica et Cosmochimica Acta 48:1135-1140

Mongin M, Molina E, Trull TW (2008) Seasonality and scale of the Kerguelen plateau phytoplankton bloom: A remote sensing and modeling analysis of the influence of natural iron fertilization in the Southern Ocean. Deep Sea Research Part II: Topical Studies in Oceanography 55:880-892

Montoya JP, McCarthy JJ (1995) Isotopic fractionation during nitrate uptake by phytoplankton grown in continuous culture. Journal of Plankton Research 17:439-464

Olson RJ, Sosik HM, Chekalyuk AM, Shalapyonok A (2000) Effects of iron enrichment on phytoplankton in the Southern Ocean during late summer: active fluorescence and flow cytometric analyses. Deep Sea Research Part II: Topical Studies in Oceanography 47:3181-3200

Pakhomov EA, Henschke N, Hunt BPV, Stowasser G, Cherel Y (2019) Utility of salps as a baseline proxy for food web studies. Journal of Plankton Research 41:3-11

Park Y-H, Roquet F, Durand I, Fuda J-L (2008) Large-scale circulation over and around the Northern Kerguelen Plateau. Deep Sea Research Part II: Topical Studies in Oceanography 55:566-581

Phillips DL, Inger R, Bearhop S, Jackson AL, Moore JW, Parnell AC, Semmens BX, Ward EJ (2014) Best practices for use of stable isotope mixing models in food-web studies. Canadian Journal of Zoology 92:823-835

Plummer M (2003) JAGS: a program for analysis of Bayesian graphical models using Gibbs sampling. Proceedings of the 3rd International Workshop on Distributed Statistical Computing 124:1-10

Post DM (2002) Using stable isotopes to estimate trophic position: models, methods, and assumptions. Ecology 83:703-718

Quezada-Romegialli C, Jackson AL, Hayden B, Kahilainen KK, Lopes C, Harrod C (2018) tRophicPosition, an r package for the Bayesian estimation of trophic position from consumer stable isotope ratios. Methods in Ecology and Evolution 9:1592-1599

R Core Team (2020) R: A language and environment for statistical computing. R Foundation for Statistical Computing, Vienna, Austria URL https://wwwR-projectorg/

Razouls S, Koubbi P, Mayzaud P (2006) Spatio-temporal distribution of mesozooplankton in a sub-Antarctic coastal basin of the Kerguelen Archipelago (southern Indian Ocean). Polar Biology 16:581-587

Schmidt K, Atkinson A, Stuebing D, McClelland JW, Montoya JP, Voss M (2003) Trophic relationships among Southern Ocean copepods and krill: Some uses and limitations of a stable isotope approach. Limnology and Oceanography 48:277-289

Semelkina AN (1993) Development of the zooplankton in the Kerguelen islands region in the years 1987-1988. In: Duhamel G (ed) Campagnes SKALP 1987 et 1988 aux iles Kerguelen à bord des navires "SKIF" et "KALPER". Publication of the Institut Français pour la Recherche et la Technologie Polaire, I0FRTP, Plouzane

Sheldon RW, Prakash A, Sutcliffe WH, Jr. (1972) The Size Distribution of Particles in the Ocean. Limnology and Oceanography 17:327

Smyntek PM, Teece MA, Schulz KL, Thackeray SJ (2007) A standard protocol for stable isotope analysis of zooplankton in aquatic food web research using mass balance correction models. Limnology and Oceanography 52:2135-2146

Sommer U, Stibor H, Katechakis A, Sommer F, Hansen T (2002) Pelagic food web configurations at different levels of nutrient richness and their implications for the ratio fish production: primary production. Hydrobiologia 484:11-20

Stowasser G, Atkinson A, McGill RAR, Phillips RA, Collins MA, Pond DW (2012) Food web dynamics in the Scotia Sea in summer: A stable isotope study. Deep Sea Research Part II: Topical Studies in Oceanography 59-60:208-221

Sunda WG, Huntsman SA (1997) Interrelated influence of iron, light and cell size on marine phytoplankton growth. Nature 390:389-392

Tarling GA, Stowasser G, Ward P, Poulton AJ, Zhou M, Venables HJ, McGill RAR, Murphy EJ (2012) Seasonal trophic structure of the Scotia Sea pelagic ecosystem considered through biomass spectra and stable isotope analysis. Deep Sea Research Part II: Topical Studies in Oceanography 59–60:222

Trull TW, Davies DM, Dehairs F, Cavagna AJ, Lasbleiz M, Laurenceau-Cornec EC, d'Ovidio F, Planchon F, Leblanc K, Quéguiner B, Blain S (2015) Chemometric perspectives on plankton community responses to natural iron fertilisation over and downstream of the Kerguelen Plateau in the Southern Ocean. Biogeosciences 12:1029-1056

Uitz J, Claustre H, Gentili B, Stramski D (2010) Phytoplankton class-specific primary production in the world's oceans: Seasonal and interannual variability from satellite observations. Global Biogeochemical Cycles 24:GB3016, doi:3010.1029/2009GB003680

Vander Zanden MJ, Rasmussen JB (2001) Variation in δ^{15}N and δ^{13}C trophic fractionation: Implications for aquatic food web studies. Limnology and Oceanography 46:2061-2066

Vargas CA, Madin LP (2004) Zooplankton feeding ecology: clearance and ingestion rates of the salps *Thalia democratica*, *Cyclosalpa affinis* and *Salpa cylindrica* on naturally occurring particles in the Mid-Atlantic Bight. Journal of plankton research 26:827-833

Verity PG, Smetacek V (1996) Organism life cycles, predation, and the structure of marine pelagic ecosystems. Marine Ecology Progress Series 130:277-293

Williams A, Koslow JA (1997) Species composition, biomass and vertical distribution of micronekton over the mid-slope region off southern Tasmania, Australia. Marine Biology 130:259-276
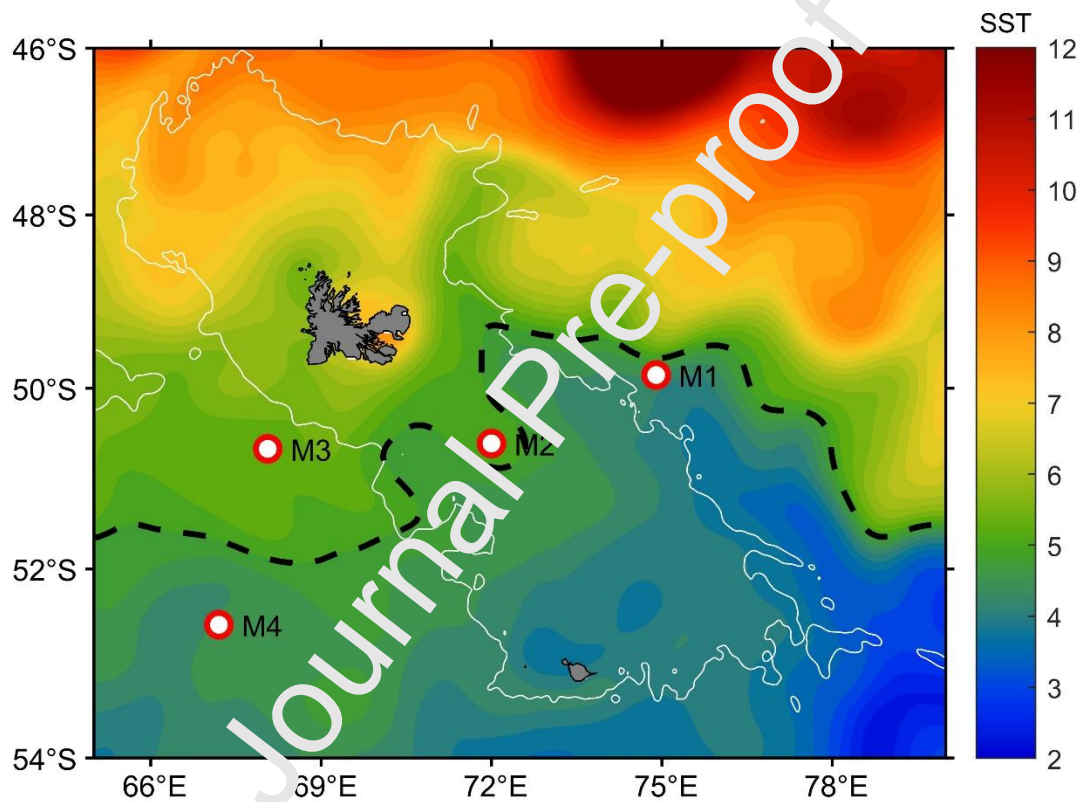
Figure 1. Map of stations sampled during the MOBYDICK expedition, from 26 February to 19 March 2018. The black dashed line indicates the position of the surface 5°C isotherm, the approximate positon of the northern branch of the Polar Front (Cotte et al., this issue). SST data were retrieved using the Copernicus platform (http://marine.copernicus.eu). Data were produced by running the OSTIA system, a merged, multi-sensor L4 Foundation SST product,

with a spatial resolution of 0.05 degrees (Donlon et al. 2012). The continental slope (continuous

white line, 1000 m isobath) and the Polar Front (dashed black line, 5°C SST) are represented.
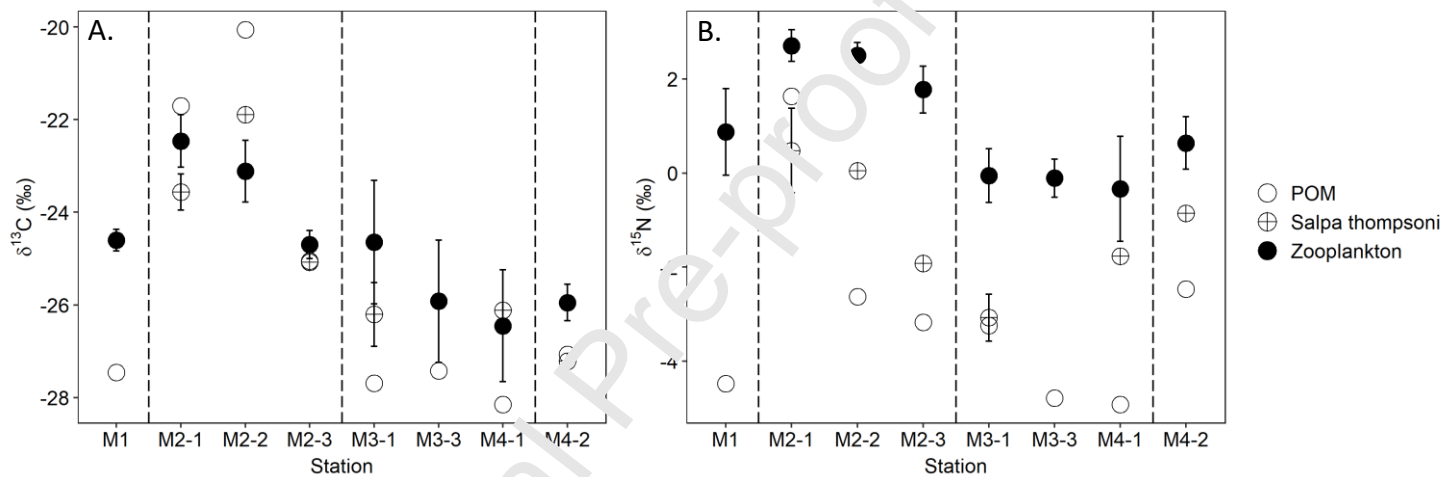

Figure 2. Values of δ^{13}C (A) and δ^{15}N (B) for trophic baseline indicators on each visit to

MOBYDICK stations M1, M2, M3 and M4, including Particulate Organic Matter (POM), the

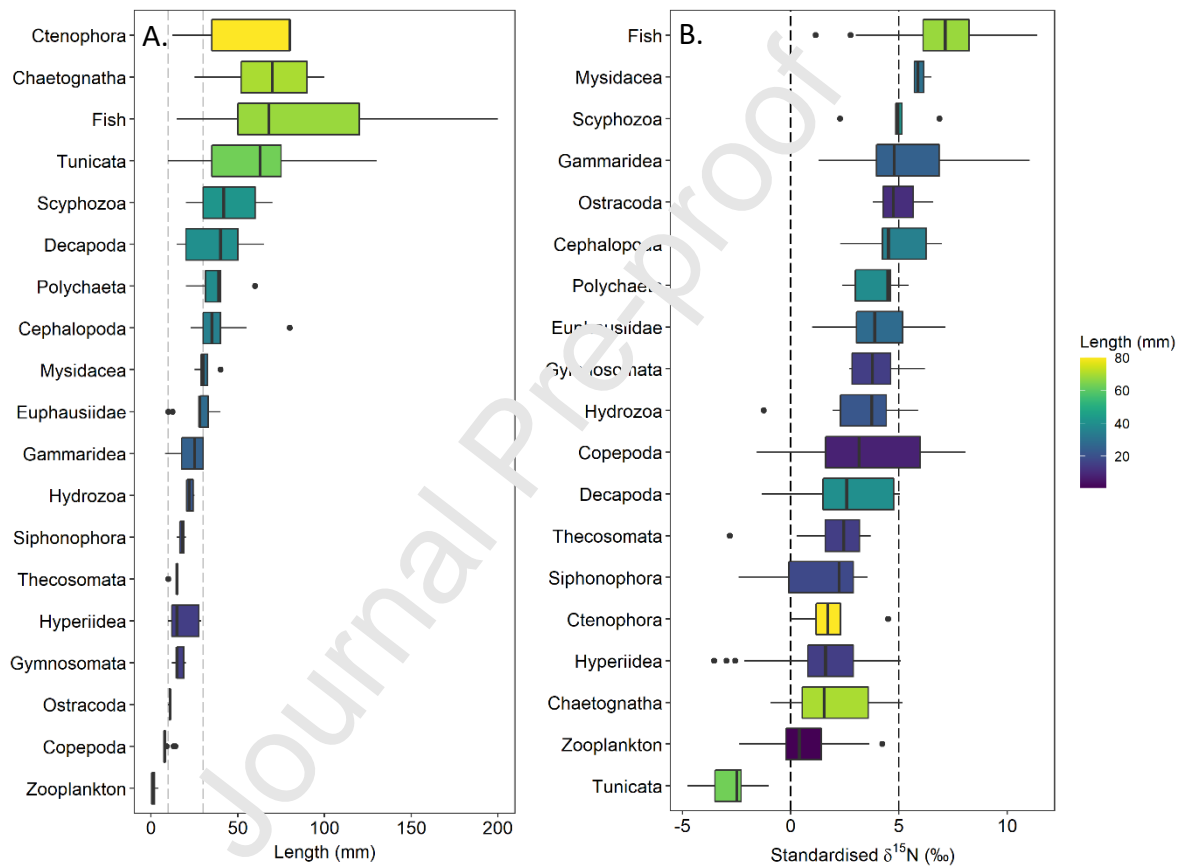tunicate *Salpa thompsoni*, and zooplankton size class ≤ 1000 µm. Error bars are standard

deviations.

Figure 3. Length (mm) (A) and standardized δ^{15}N (B) of major taxonomic groups across all stations sampled (M1, M2, M3, M4) during MOBYDICK. The vertical lines in Figure 3A indicate the separation of pelagic organisms into mesozooplankton (125 μm to ≤ 10 mm), macrozooplankton (10 - 30 mm), and micronekton (> 30 to 200 mm). Standardized δ^{15}N was calculated by setting the baseline (mean δ^{15}N of < 1000 μm zooplankton size fractions) at each

30

station to 0 ‰, and adjusting all individual organism values within a station to this baseline.

Zooplankton in the figure refers to mesozooplankton size classes ≤ 2000 μm. The largest

zooplankton size fraction (≥ 4000 μm) was separated to species during processing, and sorted

to major taxonomic groups in this figure. Tunicata were *Salpa thompsoni*. Vertical bars in the

boxplots indicate median proportional biomass. The upper and lower edges of the box denote

the approximate 1st and 3rd quartiles, respectively. The vertical error bars extend to the lowest

and highest data value inside a range of 1.5 times the inter-quartile range, respectively. Points
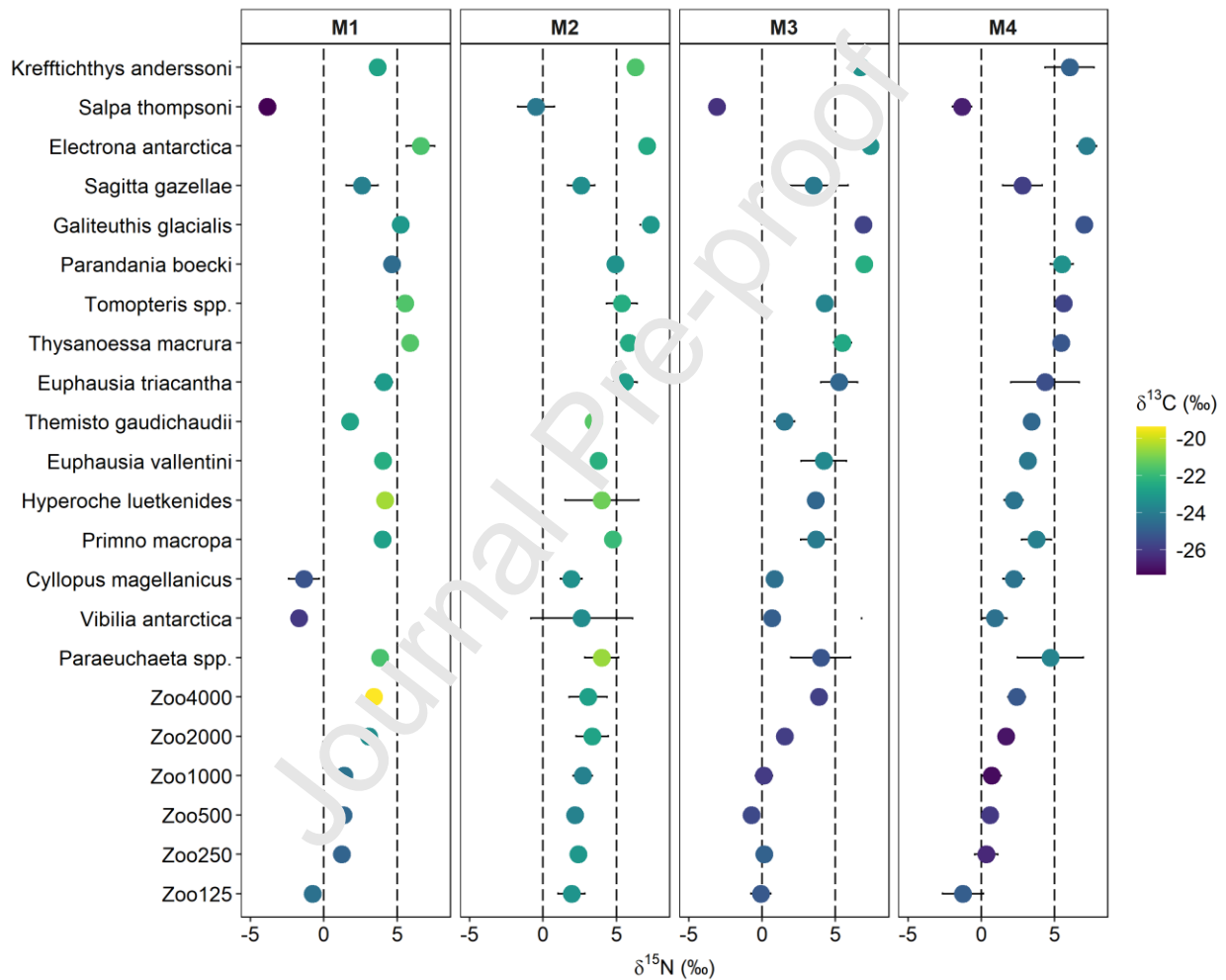
indicate extreme values.

Figure 4. Mean δ^{15}N values (± standard deviations) at stations M1, M2, M3 and M4 for taxonomic groups that were common between all stations sampled, including *Salpa thompsoni*.

Taxa are arranged on the y-axis in increasing mean size. Points are colour scaled by δ^{13}C and the dashed lines indicates δ^{13}C values of 0 and 5 ‰.
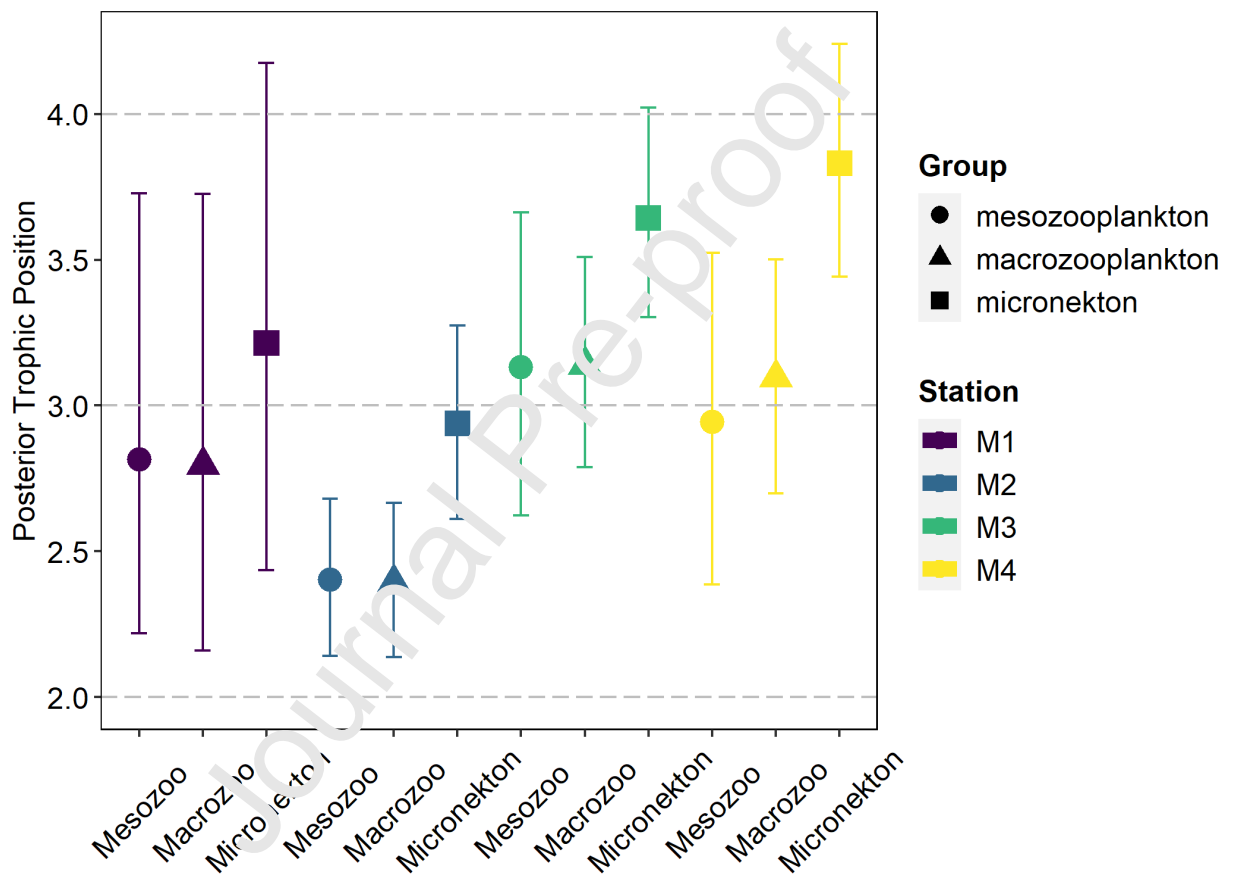

Figure 5. Posterior trophic positions (median ± 95% credibility intervals) of mesozooplankton (125 μm to 10 mm), macrozooplankton (10 - 30 mm), micronekton (> 30 mm) sampled at stations M1-M4 during the MOBYDICK survey.

Table 1. Stations sampled, with dates, depths and gears deployed. ND – No Data

Station	Date	POM	WP2+3	n_{wp2+3}	Trawl	n_{trawl}	Trawl Depths
M1	8 Mar	1	Yes	1	Yes	5	50, 400, 632, 617, 50-632
M1	9 Mar	1	No	0	Yes	1	35, 180, 340, 350, 350-0
M2-1	26 Feb	1	Yes	1	Yes	4	50, 160, 170, 310
M2-2	7 Mar	1	Yes	1	Yes	5	70, 200, 350, 70-350
M2-3	16 Mar	1	Yes	1	Yes	3	360, 400, 460, 610
M3-1	15 Mar	1	Yes	1	Yes	4	650, 800, 810, 55-460
M3-2	18 Mar	1	Yes	1	Yes	4	ND
M3-3	19 Mar	1	Yes	1	No	0	75, 380, 560, 575
M4-1	2 Mar	1	Yes	1	Yes	4	80, 550, 600
M4-2	14 Mar	1	Yes	1	Yes	3	50, 400, 632, 617

Table 2. Mean conditions at each station occupation during the 2018 MOBYDICK expedition. Zooplankton biomass is an average of the night and day WP2 net sample (200 m depth) at each station. Zooplankton carbon content was derived from dry weight, using a mean proportional carbon content from all size fractions of 35 %, measured during isotope analysis. Crustacean, gelatinous and fish biomass are from targeted Mesopelagos trawls, fully described in Cotté et al (in review).

Station	Date	Summer bloom	Residence time (days) [a]	MLD (m) [b]	Chl$_{MLDmean}$ (μg L^{-1}) [b]	T°C [b]	Zooplankton biomass (mgC m^{-3})	Crustacean biomass (mgC m^{-3}) [c]	Gelatinous biomass (mgC m^{-3}) [c]	Fish biomass (mgC m^{-3}) [c]
M1	08 Mar	Yes	~ 60	27	0.35	4.93	5.17	0.267	0.463	0.396
M2-1	26 Feb	Yes	> 60	62	0.27	5.10	12.15	0.252	0.755	0.066
M2-2	07 Mar	Yes	> 60	61	0.30	5.24	9.62	1.657	0.612	0.239
M2-3	16 Mar	Yes	> 60	68	0.58	4.99	12.07	0.143	0.229	0.029
M3-1	15 Mar	No	> 60	65	0.20	5.60	4.97	0.218	0.184	0.119
M3-2	18 Mar	No	> 60	79	0.14	5.31	10.43	0.280	0.012	0.014
M4-1	02 Mar	No	> 60	79	0.18	4.45	13.65	0.166	0.208	0.222
M4-2	14 Mar	No	> 60	82	0.21	4.46	7.12	0.021	0.305	0.002

a. Henschke et al. (2021); b. Irion et al. (2020); c. Cotté et al. (in review - this issue) .

Table 3. Probability that a random sample of posterior distribution of trophic position is greater (>) in a row than in a column, and vice versa. Pairwise comparison are between mesozooplankton (125 µm to ≤ 10 mm; Meso), macrozooplankton (10 - 30 mm; Macr), and micronekton (> 30 to 200 mm; Mnek) at stations M1, M2, M3, and M4. Blue shading indicates increasing (highest = 1) and yellow shading decreasing (lowest = 0) likelihood of difference in comparisons.

	M1-Meso	M1-Macr	M1-Mnek	M2-Meso	M2-Macr	M2-Mnek	M3-Meso	M3-Macr	M3-Mnek	M4-Meso	M4-Macr	M4-Mnek

M1-Meso	**0**	0.51	0.21	0.91	0.91	0.35	0.22	0.18	0.03	0.38	0.22	0.02
M1-Macr	0.49	**0**	0.22	0.87	0.87	0.36	0.23	0.20	0.04	0.38	0.24	0.02
M1-Mnek	0.79	0.78	**0**	0.97	0.98	0.76	0.58	0.57	0.15	0.72	0.61	0.08
M2-Meso	0.09	0.13	0.03	**0**	0.52	0.01	0.01	0.00	0.00	0.04	0.00	0.00
M2-Macr	0.09	0.13	0.02	0.49	**0**	0.01	0.01	0.00	0.00	0.04	0.00	0.00
M2-Mnek	0.65	0.64	0.24	0.99	0.99	**0**	0.25	0.20	0.00	0.50	0.28	0.00
M3-Meso	0.79	0.77	0.42	0.99	0.99	0.75	**0**	0.49	0.05	0.70	0.55	0.02
M3-Macr	0.82	0.80	0.43	1.00	1.00	0.80	0.51	**0**	0.02	0.72	0.57	0.01
M3-Mnek	0.97	0.96	0.86	1.00	1.00	1.00	0.95	0.98	**0**	0.98	0.98	0.25
M4-Meso	0.62	0.62	0.28	0.96	0.96	0.50	0.30	0.28	0.02	**0**	0.33	0.01
M4-Macr	0.78	0.76	0.39	1.00	1.00	0.73	0.45	0.43	0.02	0.67	**0**	0.01
M4-Mnek	0.98	0.98	0.92	1.00	1.00	1.00	0.98	0.99	0.75	0.99	0.99	**0**

Table 4. The probability of overlap of posterior distributions of trophic position (Bhattacharya coefficient) in pairwise comparison between mesozooplankton (125 µm to ≤ 10 mm; Meso), macrozooplankton (10 - 30 mm; Macr), and micronekton (> 30 to 200 mm; Mnek) at stations M1, M2, M3, and M4. Blue shading indicate increasing (highest = 1) and yellow shading decreasing likelihood (lowest = 0) of overlap in comparisons.

	M1-Meso	M1-Macr	M1-Mnek	M2-Meso	M2-Macr	M2-Mnek	M3-Meso	M3-Macr	M3-Mnek	M4-Meso	M4-Macr	M4-Mnek
M1-Meso	0.00	0.99	0.84	0.57	0.55	0.88	0.83	0.73	0.29	0.96	0.81	0.23
M1-Macr	0.99	0.00	0.86	0.63	0.61	0.85	0.84	0.73	0.33	0.96	0.80	0.26
M1-Mnek	0.84	0.86	0.00	0.30	0.28	0.77	0.96	0.89	0.65	0.90	0.91	0.52
M2-Meso	0.57	0.63	0.30	0.00	1.00	0.24	0.23	0.09	0.00	0.43	0.17	0.00
M2-Macr	0.55	0.61	0.28	1.00	0.00	0.21	0.20	0.07	0.00	0.40	0.14	0.00
M2-Mnek	0.88	0.85	0.77	0.24	0.21	0.00	0.86	0.84	0.15	0.94	0.90	0.07
M3-Meso	0.83	0.84	0.96	0.23	0.20	0.86	0.00	0.97	0.50	0.93	0.98	0.34
M3-Macr	0.73	0.73	0.89	0.09	0.07	0.84	0.97	0.00	0.38	0.87	0.99	0.21
M3-	0.29	0.33	0.65	0.00	0.00	0.15	0.50	0.38	0.00	0.34	0.36	0.89

38

Mnek												
M4-Meso	0.96	0.96	0.90	0.43	0.40	0.94	0.93	0.87	0.34	**0.00**	0.93	0.23
M4-Macr	0.81	0.80	0.91	0.17	0.14	0.90	0.98	0.99	0.36	0.93	**0.00**	0.21
M4-Mnek	0.23	0.26	0.52	0.00	0.00	0.07	0.34	0.21	0.89	0.23	0.21	**0.00**

Highlights

- This study used stable isotopes to analyse the pelagic food web structure in the Kerguelen Island region, comparing HNLC areas upstream of the plateau and the iron enriched area on the plateau that experiences a large seasonal phytoplankton bloom.
- Trophic position was calculated for mesozooplankton, macrozooplankton, and micronekton using a Bayesian isotope mixing model approach.
- Meso and macrozooplankton trophic positions were similar but ~ 0.6 trophic positions lower than micronekton within areas.
- Median meso / macrozooplankton trophic position was ~ 2.4 on the plateau and 0.6 trophic positions higher in HNLC areas.
- Food chains were longer in HNLC regions, and food chain length was determined by the composition of the trophic levels below micronekton.
- Size based food web structure was robust to differences in community taxonomic composition.
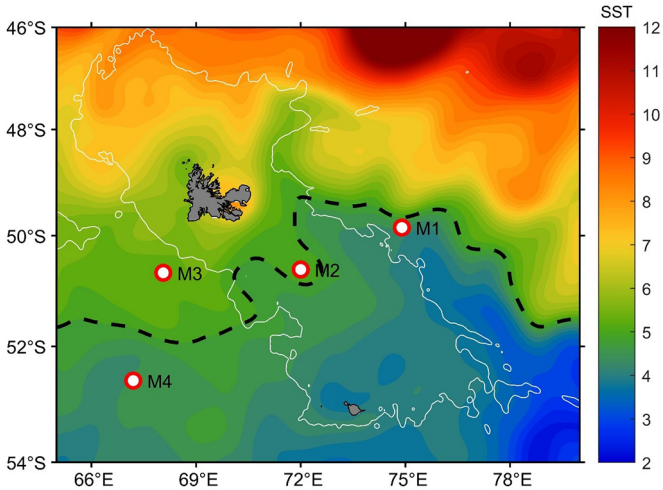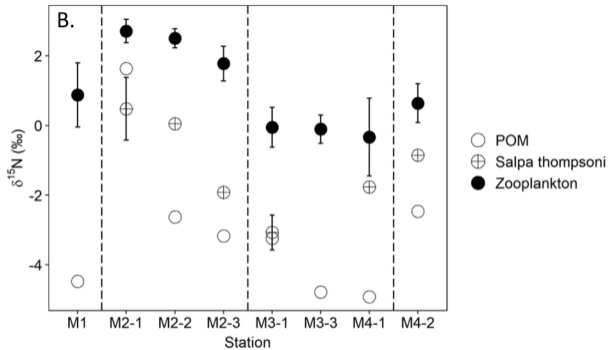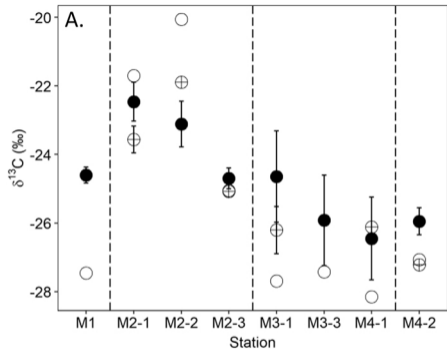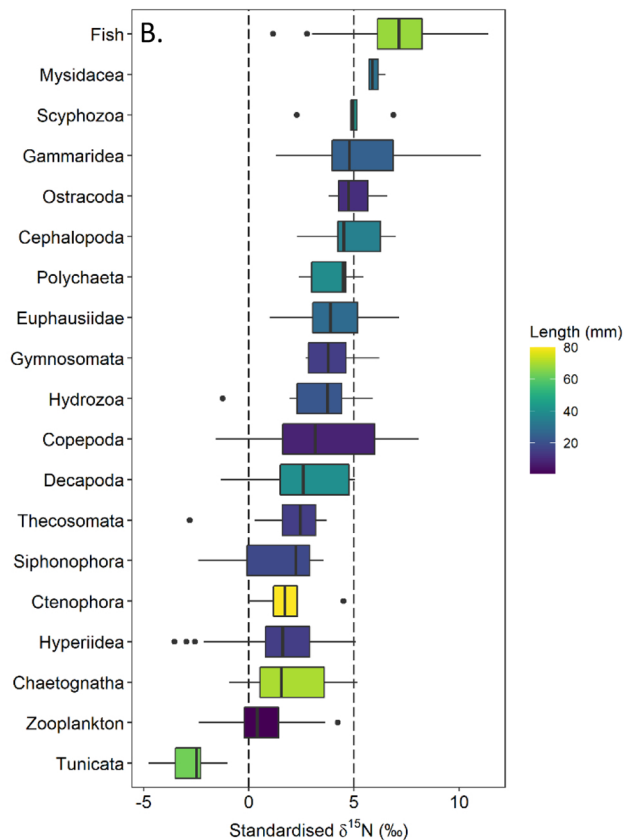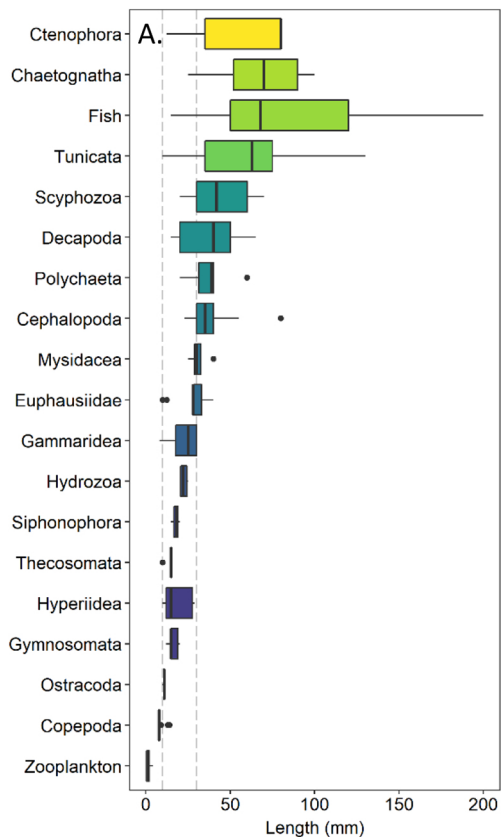
Figure 1

Figure 2

Figure 3

Figure 4

Figure 5